

Supplementary Information

Bioinspired Robust Non-iridescent Structural Color with Self-Adhesion Amorphous Colloidal Particle Arrays

Panmiao Liu, Jialun Chen, Zexi Zhang, Zhuoying Xie,* Xin Du, and Zhongze Gu*

Experimental Procedures

Materials: 3-Hydroxytyramine hydrochloride (DA) and tris(hydroxymethyl)aminomethane (Tris) were purchased from Aladdin (Shanghai, China). Ammonium hydroxide (28 wt%), ethyl alcohol was purchased from Sinopharm Chemical Reagent Company. Poly(methylmethacrylate) (PMMA) plank was purchased from Shanghai Siyun Building Materials Co. (Shanghai, China). Paper was purchased from Tongxiang Yimei Paper Industry Co. (Hunan, China). Aluminum sheet was purchased from Shenzhen Hong Jintai Array Technology Co. (Shenzhen, China). Glass slide was purchased from Nanjing Wanqing Co. (Nanjing, China). A polypropylene (PP) film (PP2910, 100 μm thick, 210 mm \times 297 mm, 3M) and transparent and double side tape (600i ROLL, 12.7 mm \times 32.9 m, 3M) were obtained from Aice Instrument. SiO_2 particles with different diameters were purchased from Nanjing Caina Biological Technology Company. Deionized water (18.0 M Ω cm, Milli-Q gradient system, Millipore) was used in all experiments. All chemical reagents were used without further purification. Sandpaper was obtained from Germany (P2000, Warrior sandpaper).

Preparation of PDA@SiO₂: PDA@SiO₂ was prepared by disperse 0.1g SiO₂ particles into 10ml DA and Tris solution (pH=7~7.5) for stirring for 18 h. Then the obtained particles were cleaned by centrifugalization for three times and further purification with filter membrane. The thickness of PDA shells was adjusted by DA concentration.

Preparation of structural color arrays: Particle solution was prepared by dispersing PDA@SiO₂ in deionized water and then ultrasonic for 10 min to form a latex suspension containing 20 wt% PDA@SiO₂. Glass slides were cut of 2.5 cm \times 2.5 cm and washed by a 50 wt% alcohol solution in an ultrasonic bath for 15 min. Then these glass slides were taken out and wiped by a dust-free paper. The structural colored arrays were fabricated by spraying the 20wt% PDA@SiO₂ aqua using an airbrush system with a 0.2-mm bore, at a pressure of 0.2 MPa. The working distance between the bore and substrate was about 10 cm. And the fabrication process of the samples was conducted at temperature of 45°C and humidity of 19%.

Preparation of structural color patterns: The structural color patterns were fabricated by spraying PDA@SiO₂ on the substrate via pattern masks. The pattern masks were designed using Auto CAD and fabricated by a laser cutter (4060, Ketai) with a PP film.

Characterization: The reflection spectrum were measured by a spectrometer (QE65000, Ocean Optics) with light source (DH-2000UV-VIS-NIR, Mikropack) and optical fiber (QR200-7-UV-BX, Ocean Optics). The absolute reflectance was measured using a diffuse reflection standard plate (WR-D97-30, Oceanhood) as completely diffuse reflector. The PDA@SiO₂ images were obtained by Field Emission Scanning Electron Microscope (FESEM, Zeiss Ultra Plus). The images of amorphous colloidal arrays were obtained by a scanning electron microscope (SEM, S-3000N, Hitachi). The microphotographs of the array were taken by the metalloscope (OLYMPUS BX51) with a CCD camera (Media Cybernetics EvolutionMP 5.0). Contact angles of substrates were measured using a CA measurement device (Powereach, Zhongchen). PDA@SiO₂ and SiO₂ amorphous arrays with 16 μm thickness were detected at normal incidence to compare the absorptivity (Fig.S3).

Fastness test: The spraying process of sample were shown in Movie S1. For the convenience of observation, the SiO₂ samples in paper substrate were doped slight PDA. The sandpaper abrasion tests were carried out by placing sample weighting 50 g face-down to sandpaper and moved for 5 cm along the ruler. The sample was then moved for 5 cm in the opposite direction along the ruler. This process is defined as one abrasion cycle (Movie S4-S7). For the convenience of observation, ultrasonic cleaning test, shown in Movie S3, was conducted in the bottom of ultrasonic instrument with the SiO₂ arrays, PDA@SiO₂ arrays, and PDA@SiO₂-AM arrays.

Lap shear test: All samples were prepared on the glass. In the case of tape-tearing test, curing 3M transparent tapes (12.7 mm \times 32.90 mm) on the samples surface with full adhesion. The tape is torn back from the surface of the sample under uniaxial tensile at a rate of 2 mm/min using a universal testing machine (UTM) for 20 min.^[1] In the case of cohesive failure tensile test, curing 3M double side tape (1 cm \times 1 cm) on the samples surface with full adhesion. Uniaxial tensile was applied to the samples at a rate of 2 mm/min until the samples separated from the substrate.

Calculation of retaining area ratio: The area of square arrays was 1 cm \times 1cm and matched 10 \times 10 grids. The area ratio of retain array was measured by counting the grids number (grid area of more than 50% was regard as one grid number) of the retain array area and then dividing the total (100).

S1 PDA@SiO₂ particles

These were determined by particle size distribution histogram measured from one hundred particles with an average diameter of 295 nm and the PDI is 0.026. Raman spectras of SiO₂ particles and PDA@SiO₂ (Fig.S1b) are shown that the characteristic bands of SiO₂ particles are in the range of 500 and 2490 cm⁻¹. While PDA@SiO₂ samples spectra appeared two strong bands at 1355 and 1579 cm⁻¹, which can be assigned to the deformation of the catechol group in the PDA structure. These indicated that the PDA coated on SiO₂ particles. The PDA levels of PDA@SiO₂ depended on the original concentration of DA in the oxidation self-polymerization reactive system. PDA@SiO₂ with different content of PDA were prepared using the DA concentration of 1 mM, 5 mM, 10 mM and 20 mM in 10 ml solution containing concentration of 0.02 g/ml SiO₂ particles with diameter of 275 nm, respectively. The results were shown in Fig. S1c that a small number of PDA granular was attached to the surface of SiO₂ particles when the DA concentration is low. While when the DA concentration was reached 0.01 M, the PDA granular were conglomerated each other and then generated PDA shells. And the final diameter of the obtained PDA@SiO₂ ranging from 275~320 nm is linear to the original DA concentration, as shown in Fig.S5b. The phenomenon may be explained by formation mechanism of PDA.^[2,3] The formation of PDA could be adjusted by pH of reaction condition. When the pH was low (lower than 7.5), more quinone structures existed in the final PDA mixture. The hydrophobic of quinone therefore resulted in more PDA granulars generation. For the PDA coating SiO₂ particles reaction, the low pH not only makes PDA tend to granulars to adhere SiO₂, but also lower the reaction speed, which makes the PDA efficiently coated on the surface of SiO₂ and avoid redundant granulars in solution. The contrast results of lower pH and higher pH that PDA coated SiO₂ particles are showed in Fig.S1f.

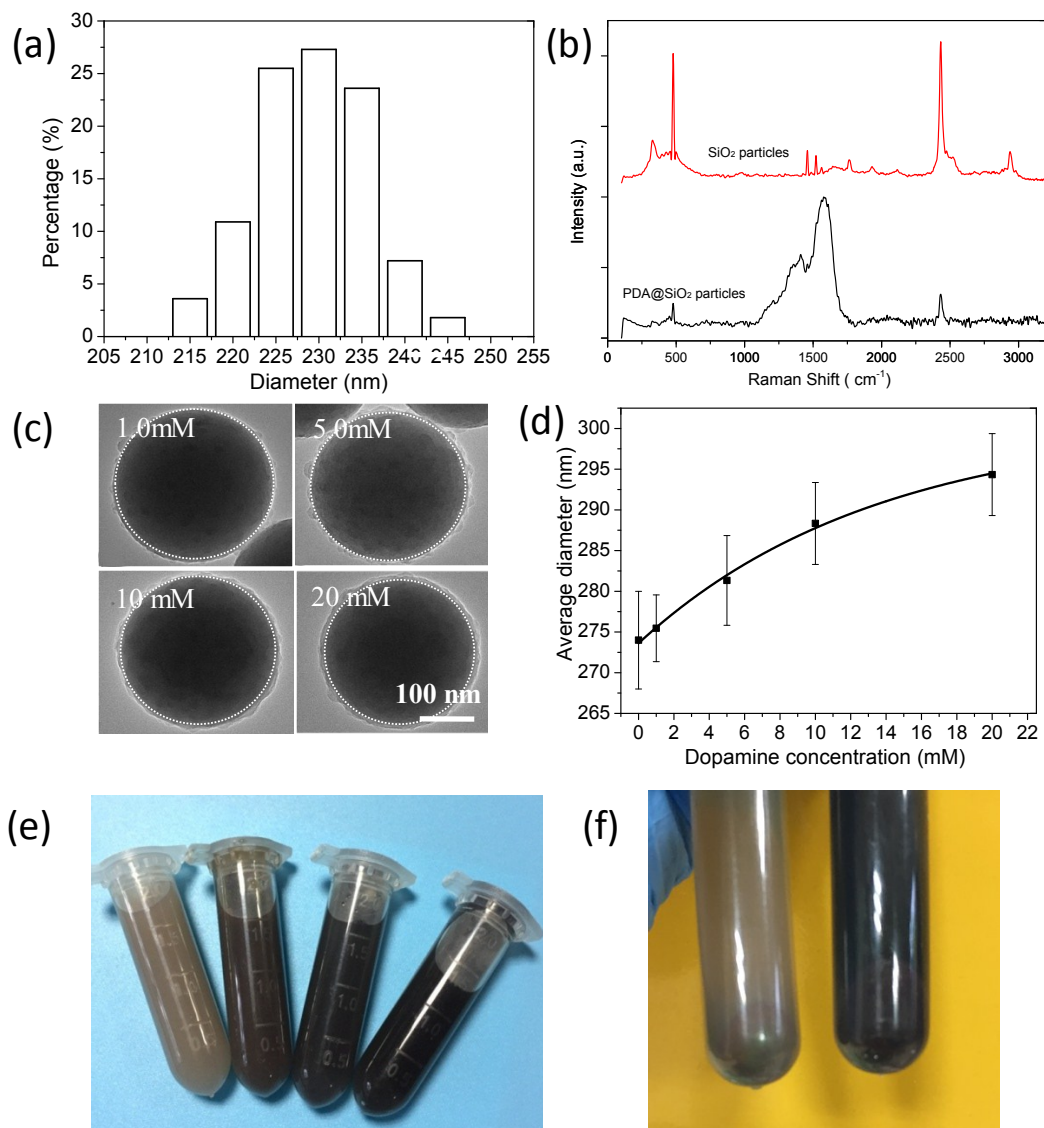


Fig. S1 (a) Particle size distribution histogram measured from one hundred particles in TEM images with an average diameter of 232 nm PDA@SiO₂. (b) Raman spectras of SiO₂ particles and PDA@SiO₂. (c) TEM images of PDA@SiO₂ synthesized by the same size SiO₂ particles and different dopamine content, using the dopamine concentration of 1.0 mM, 5.0 mM, 10 mM and 20 mM in 10 ml solution containing concentration of 0.02 g/ml SiO₂ particles with diameter of 275 nm, respectively. The white dotted circle presented the SiO₂ core. (d) The relationship between diameter of PDA@SiO₂ and the dopamine concentration. (e) Photographs of obtained PDA@SiO₂ solution with the gradual increment of DA initial concentration of 1 mM, 5 mM, 10 mM and 20 mM. (f) Compared photographs of obtained PDA@SiO₂ solution with different pH reaction conditions (the left sample is synthesized at pH =7, and the right sample is synthesized at pH= 9).

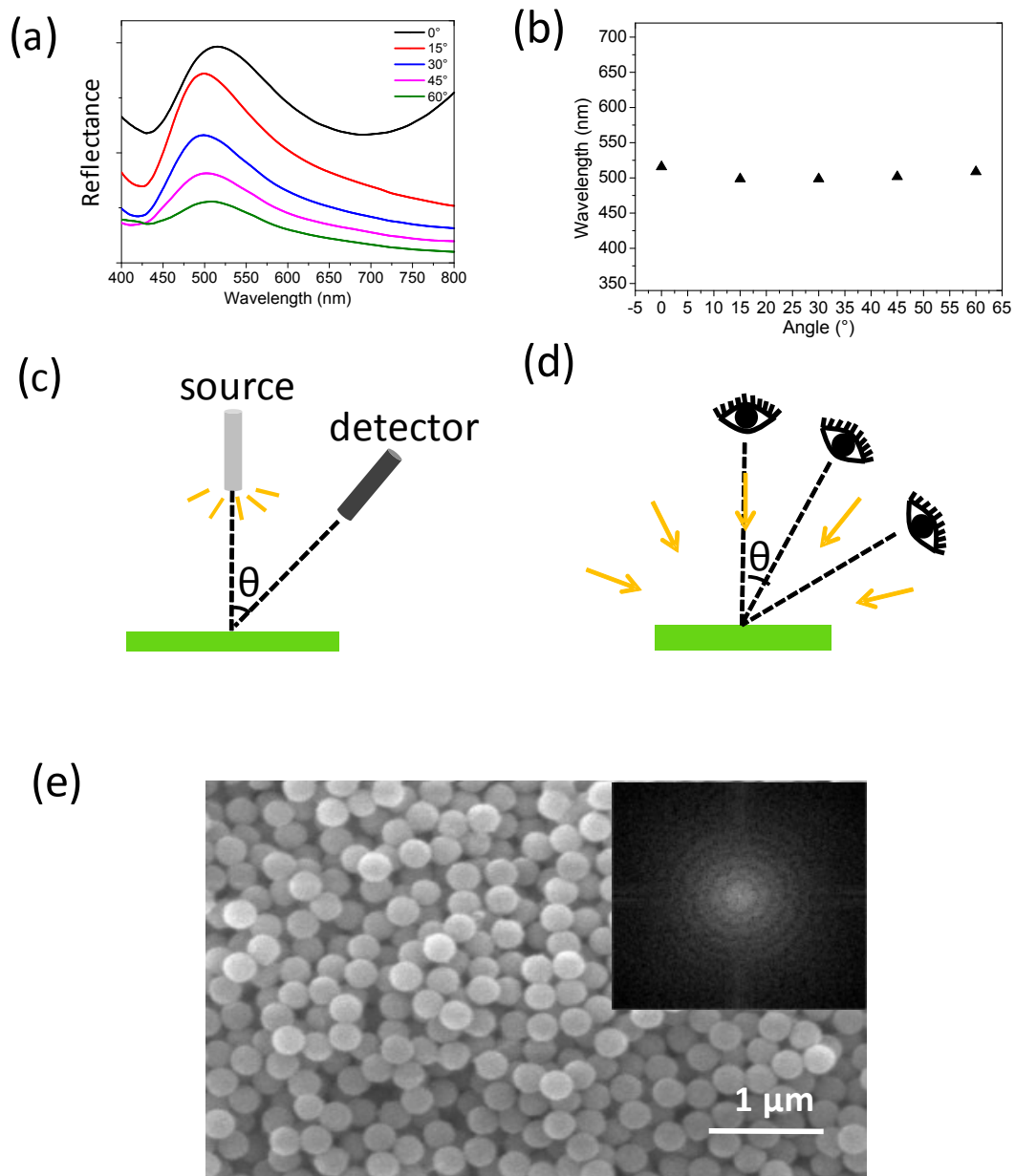


Fig. S2 (a) Reflection spectra of 232 nm PDA@SiO₂ arrays at various detected angles. (b) Reflectance positions for the green arrays on different detected angles. (c) Schematic diagram of the optical detection at different angles and the incident angle relative to the normal membrane surface was 0°. (d) Schematic diagram of photographs at different viewing angles under diffusive lighting conditions. (e) SEM image assembled the amorphous array with an average diameter of 232 nm and its two-dimensional Fourier analyses (the insert image).

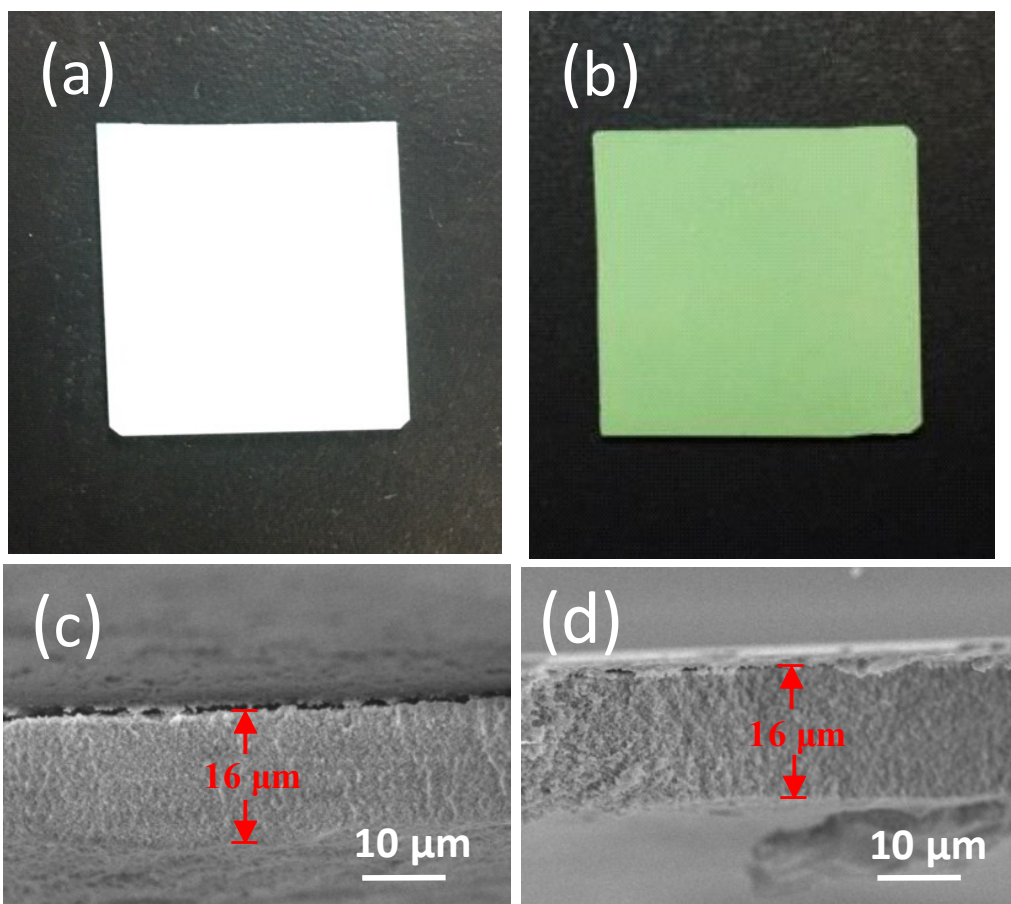


Fig. S3 (a,b) The images of SiO_2 and PDA@SiO_2 array fabricated with 232 nm SiO_2 and PDA@SiO_2 particles, respectively. (c,d) SEM image of cross section of SiO_2 and PDA@SiO_2 arrays with 16 μm thickness.

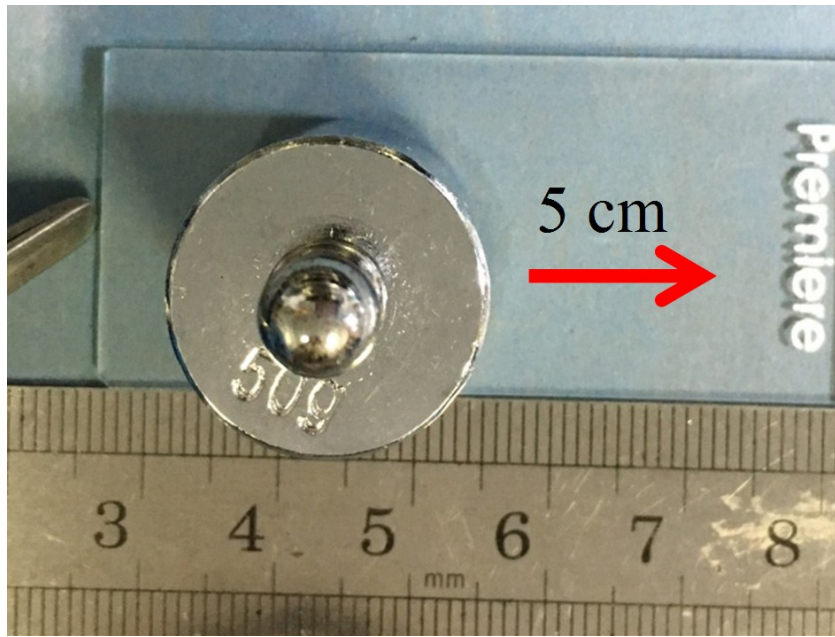
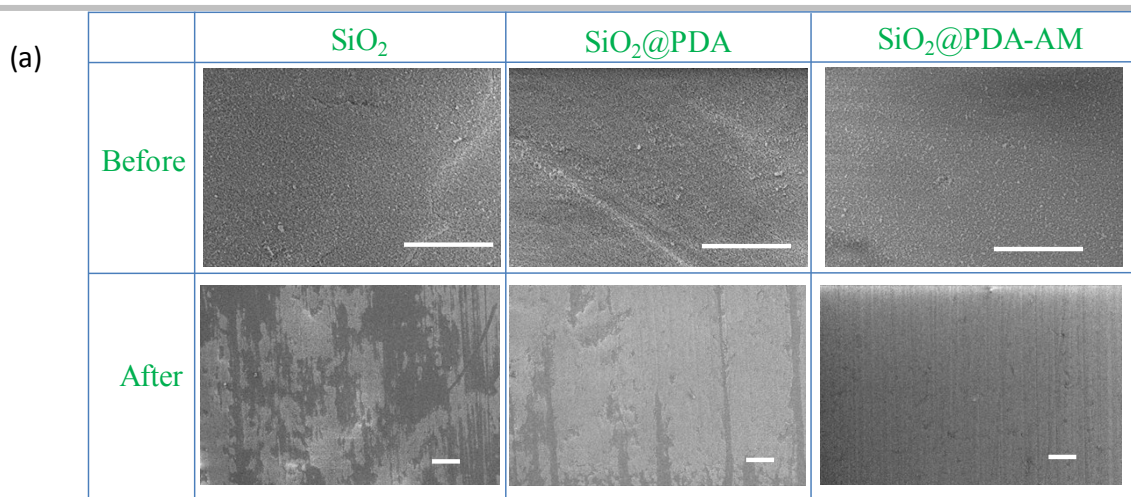


Fig. S4 Process of the sandpaper abrasion test for the glass sample.



(b)

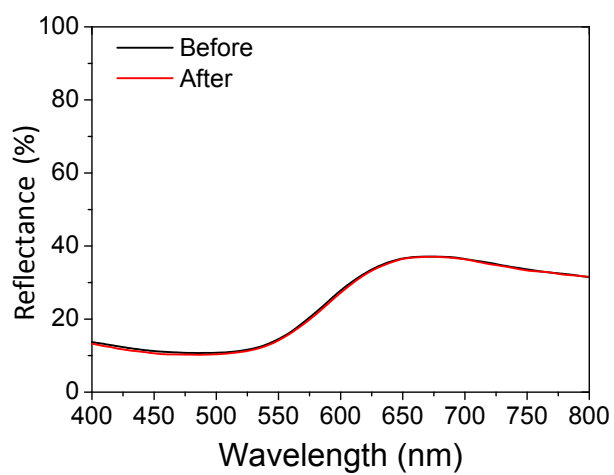


Fig. S5 (a) SEM images of SiO₂, PDA@SiO₂ and PDA@SiO₂-AM arrays before and after sandpaper abrasion test. The insert scale bar is 100 μm. (b) The reflection spectra before and after sandpaper abrasion tests for PDA@SiO₂-AM arrays.

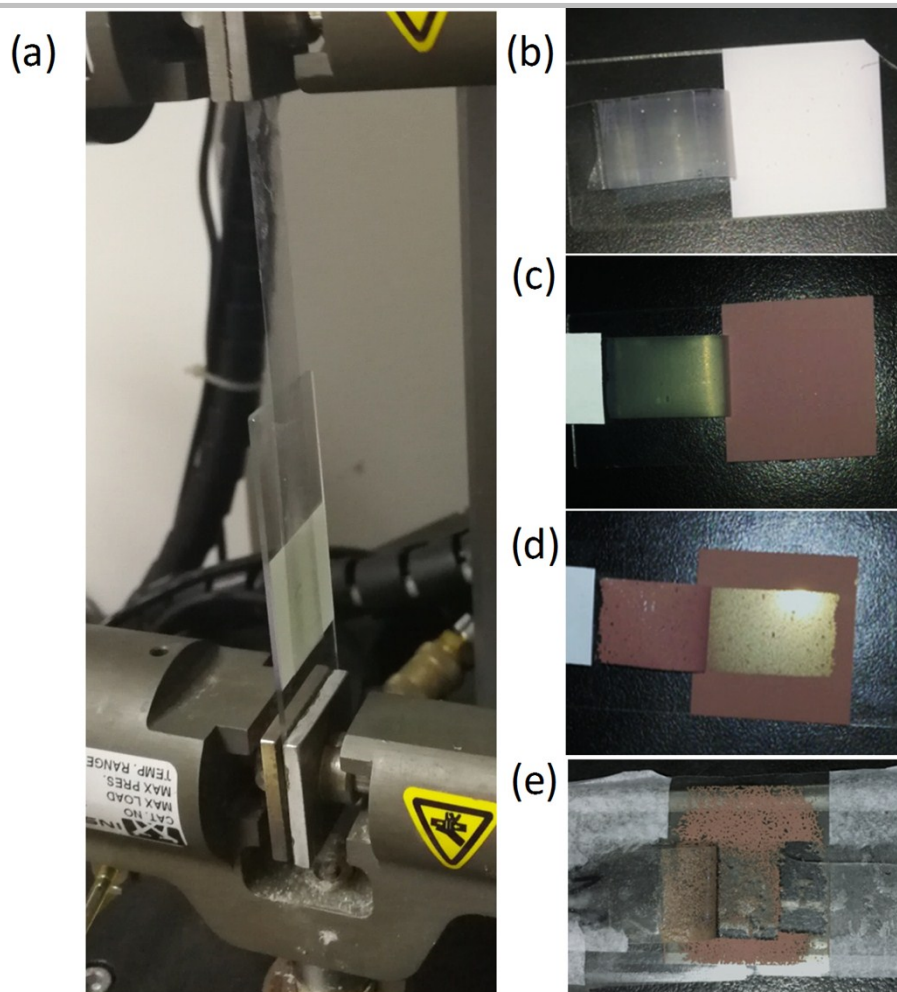


Fig. S6 (a) Photograph of lap-shear test by tape-tearing form of SiO_2 arrays. (b-d) Photographs of SiO_2 , PDA@SiO_2 and $\text{PDA@SiO}_2\text{-AM}$ arrays after tape-tearing test on glass substrate. (e) Photograph of $\text{PDA@SiO}_2\text{-AM}$ arrays after tape-tearing test on tape substrate.

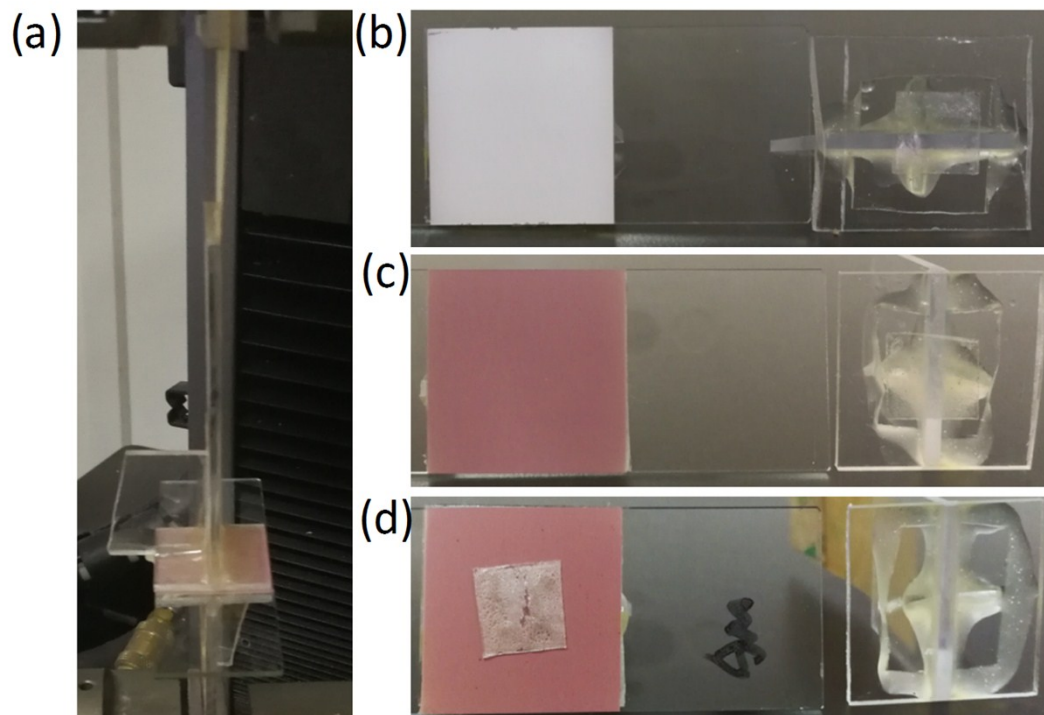


Fig. S7 (a) Photograph of lap-shear test of cohesive failure tensile of PDA@SiO₂ arrays. (b-d) Photographs of SiO₂, PDA@SiO₂ and PDA@SiO₂-AM arrays after cohesive failure tensile test on glass substrate.

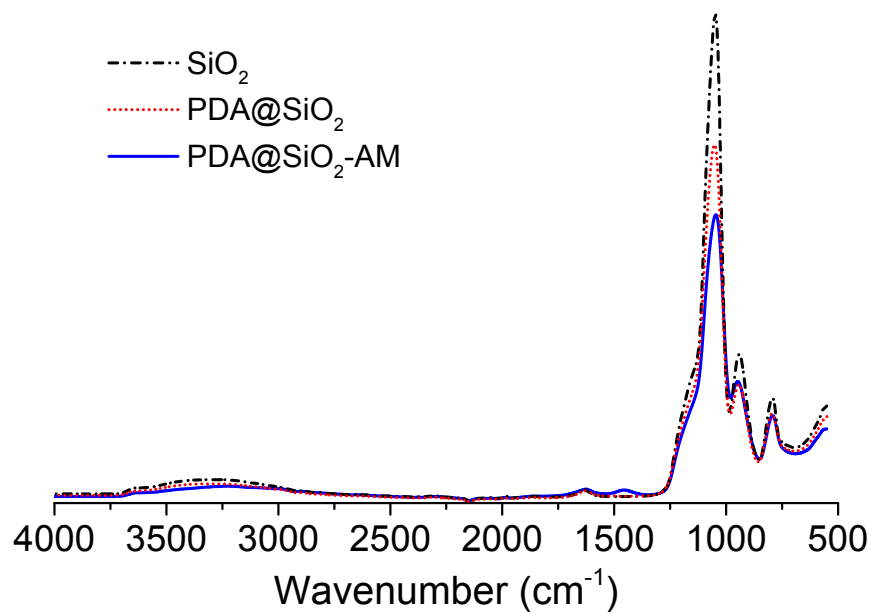


Fig. S8 ATR-IR spectrum of PDA@SiO₂-AM, PDA@SiO₂ and SiO₂ arrays.

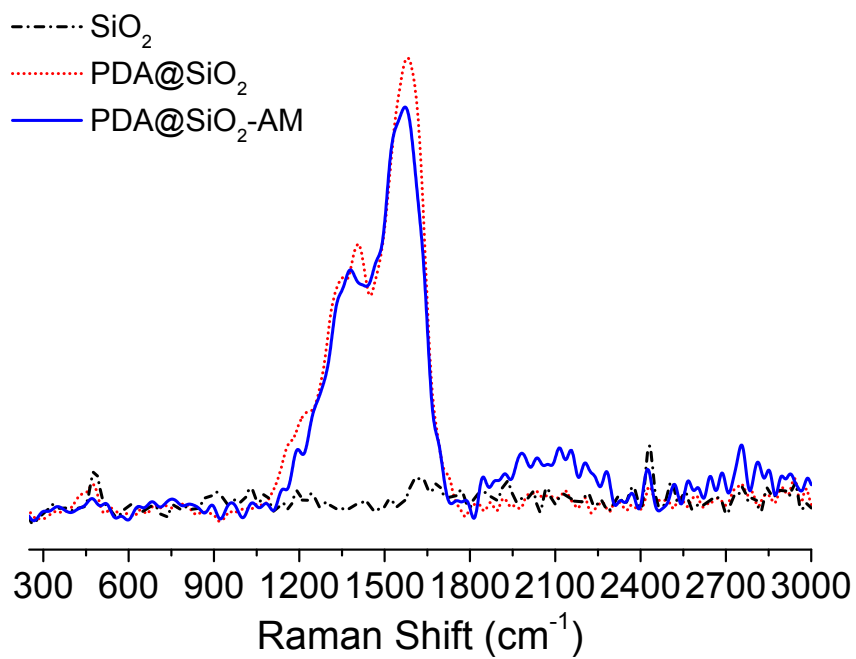


Fig. S9 Raman spectrum of PDA@SiO₂-AM, PDA@SiO₂ and SiO₂ arrays.

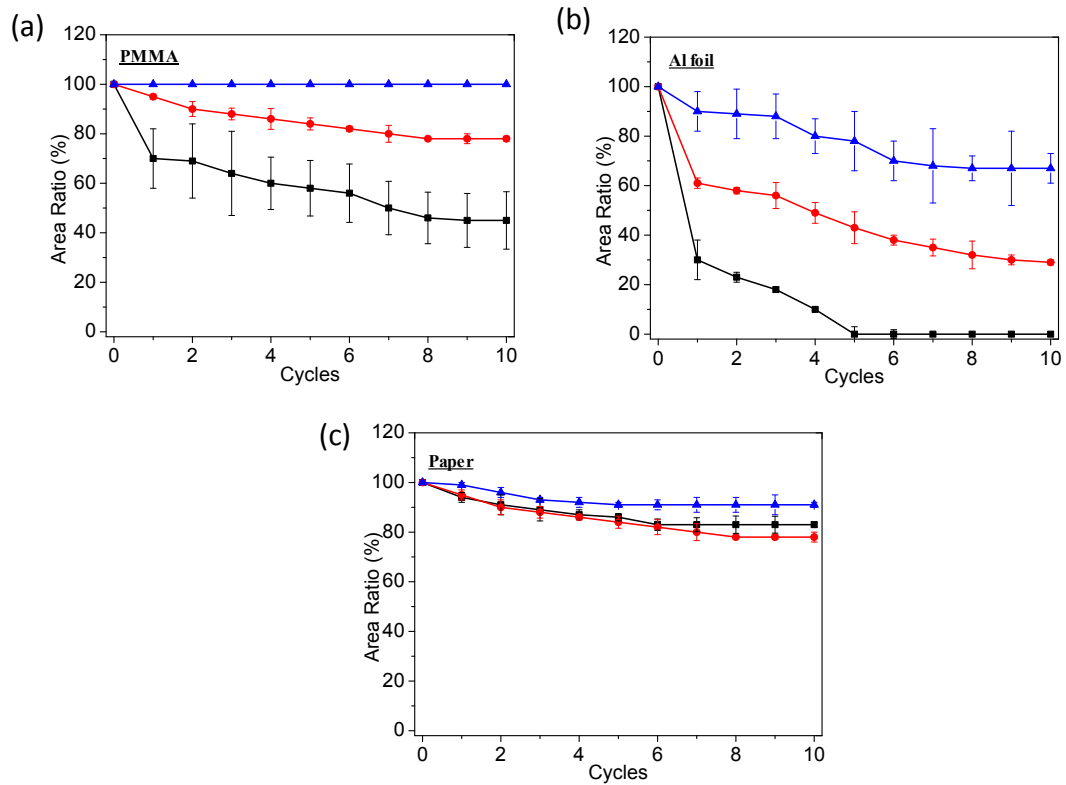


Fig. S10 Retaining area ratio during the test of sandpaper abrasion test of SiO₂ (square), PDA@SiO₂ (circle) and PDA@SiO₂-AM (triangle) arrays on PMMA (b), Al foil (c) and paper (d) substrate, respectively.

(a)



(b)



(c)



(d)



Fig. S11 The contact angles of (a) glass ($36.3 \pm 0.1^\circ$), (b) PMMA ($71.3 \pm 0.5^\circ$), (c) Al foil ($96.5 \pm 0.2^\circ$) and (d) paper (0°) substrates.

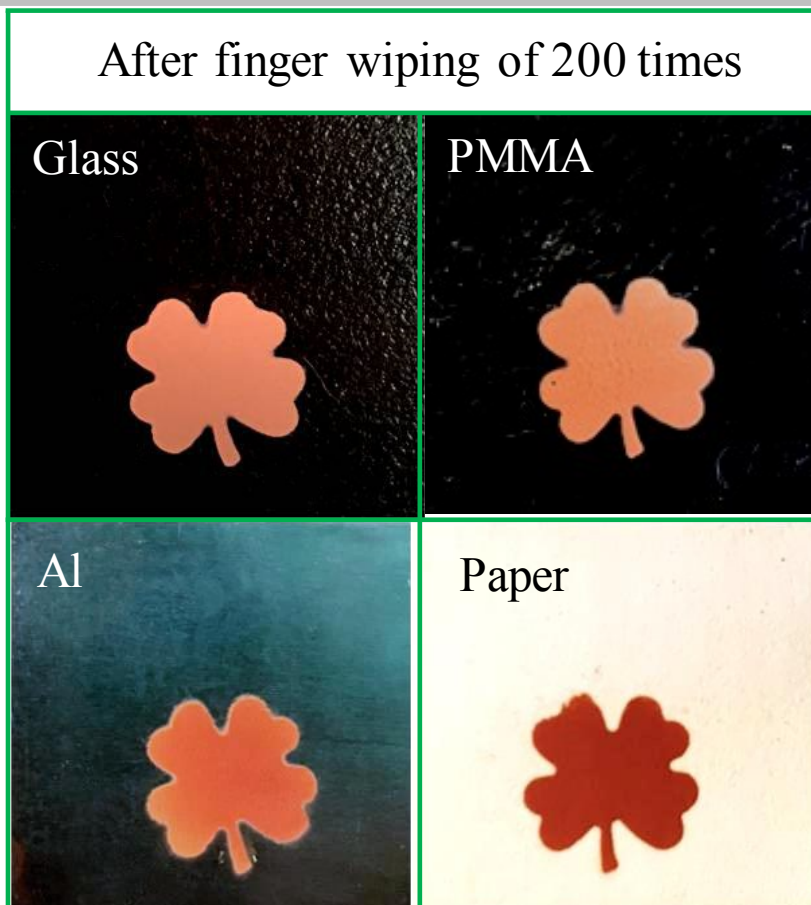


Fig. S12 Photographs of PDA@SiO₂-AM arrays with clover shape on glass, PMMA, Al foil and paper substrates after 200 times finger-wipe.

S13. Color theory and calculation of three tristimulus values

Color is a perception of the human eye vision system to light. The CIE 1931 color spaces were the first defined quantitative links between physical pure colors in the electromagnetic visible spectrum, and physiological perceived colors in human color vision. The mathematical relationships that define these color spaces are essential tools for color management. For colored measurement, electromagnetic visible spectrum was defaulted to absolute reflection spectra, obtained with the calibration standard whiteboard as completely diffuse reflector. Absolute reflectance is a bridge of the visual color to the color data, so-called tristimulus values (CIE XYZ), calculated by the CIE's color matching functions. Tristimulus values (CIE XYZ) are the three parameters that correspond to the levels of stimulus of three types of cone cells in the retina of the human eyes to the light of certain wavelengths in the visible region, which peaks at approximately 430 nm, 540 nm, and 570 nm. The CIE XYZ color space is deliberately designed that the Y parameter is a measure of the luminance of a color. The chromaticity of a color is then specified by the two derived parameters x and y, two of the three normalized values being functions of all three tristimulus values X, Y, and Z. The derived color space specified by x, y, and Y is known as the CIE xyY color space and is widely used to specify colors in practice.

All color sensations are in principle endowed with inherent tristimulus values (CIE XYZ), which could be used for the evaluation of three attributes of color: hue, luminance and saturation. Among them, hue presents the appearance of a color and is represented by the dominant wavelength in the CIE xyY color space. Dominant wavelength is wavelength of spectral trajectory sited on the intersection point of chromaticity parameter (x, y) of this color with the spectral trajectory. Luminance of a color specifies the lightness of the color. In the CIE xyY color space, Y parameter is a measure of this attribute. Saturation denotes the purity of a color. In the CIE xyY color space, the quantitative value to specify this property is calculated as follows:

$$S = \frac{X_{\lambda} + Y_{\lambda} + Z_{\lambda}}{X + Y + Z}$$

In the formula, X, Y and Z are the three tristimulus values of this color and X_{λ} , Y_{λ} and Z_{λ} are the tristimulus values of the corresponding dominant wavelength sited in the spectral trajectory.

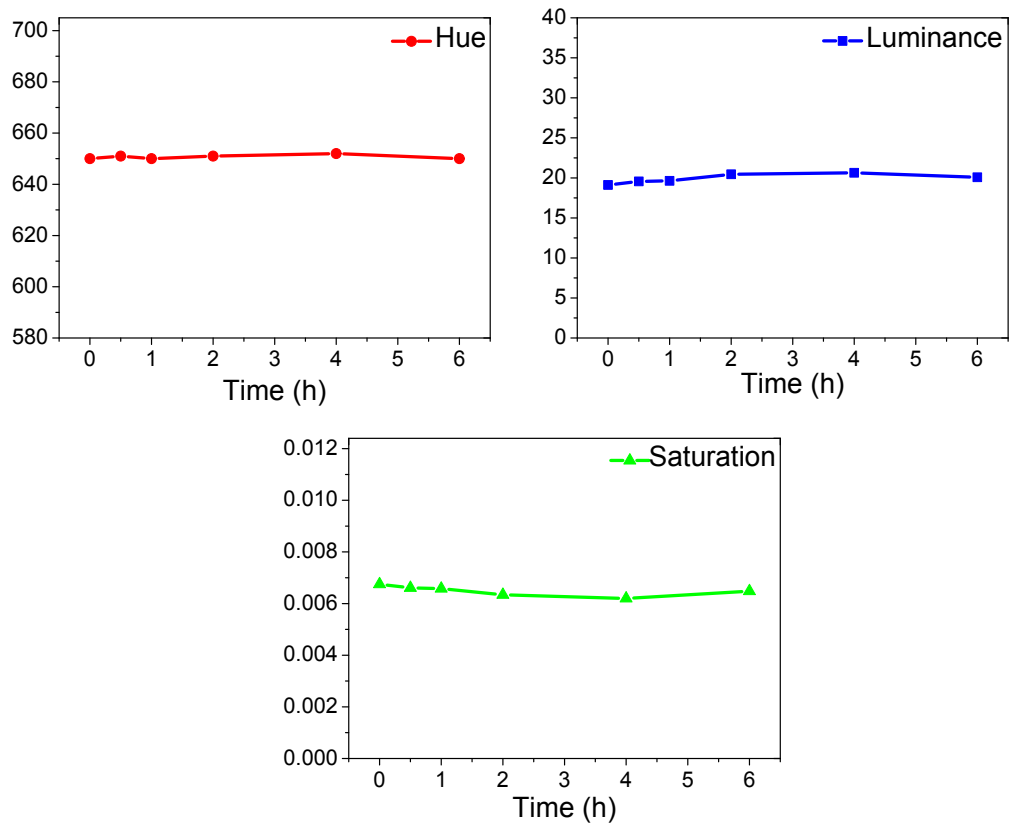


Fig. S13 The changing of Hue, Luminance and Saturation of PDA@SiO₂ arrays on glass with different treatment time by ammonium vapor of 20 wt%.

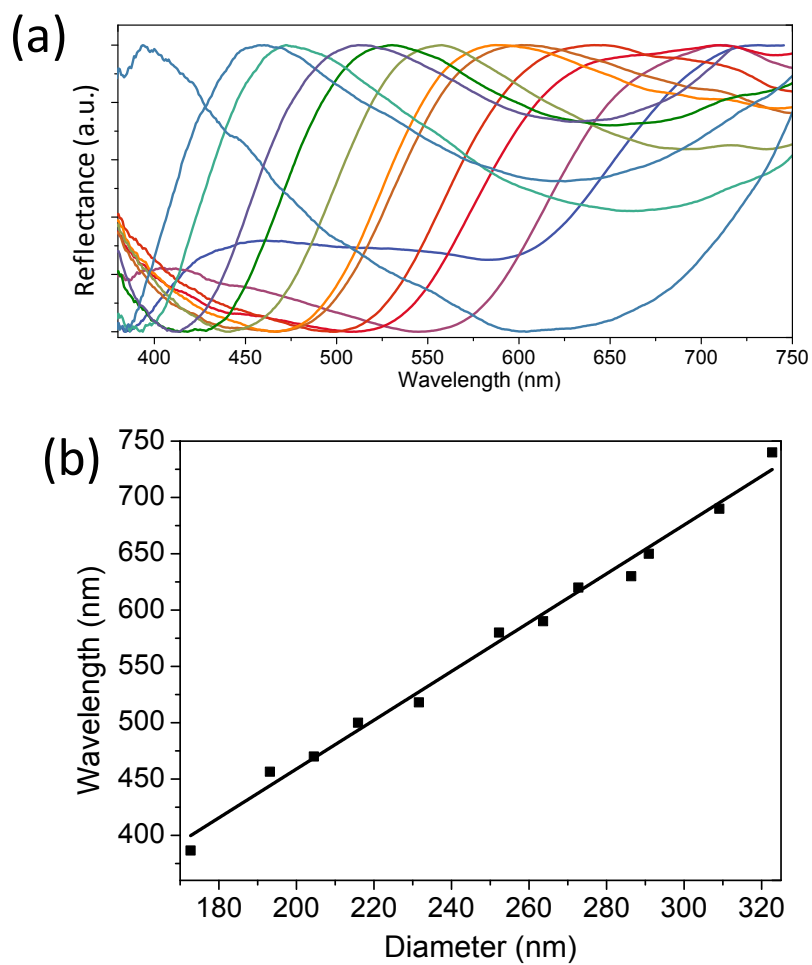


Fig. S14 (a) The normalized reflectance spectra of the PDA@SiO₂ arrays with particle sizes of 175, 195, 208, 218, 232, 252, 264, 273, 286, 295, 309 and 323 nm composed of silica core with 168, 188, 201, 211, 225, 245, 257, 266, 279, 288, 302 and 316 nm size and all the PDA shell with 7 nm. (b) The relationship between the diameter and dominant reflection wavelength of the arrays.

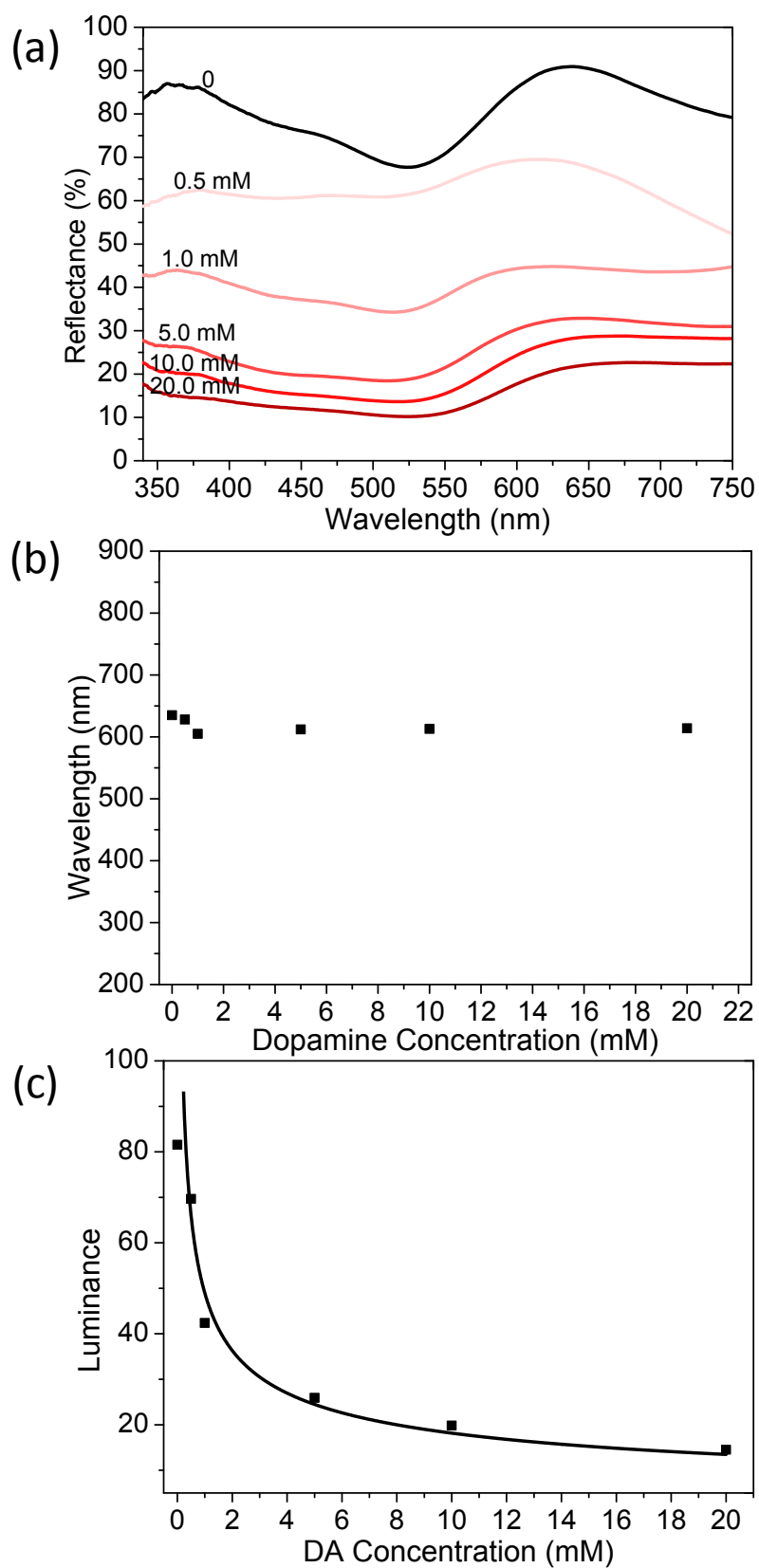


Fig. S15 (a) Reflection spectrum of the arrays with different dopamine concentration. (b) The corresponding reflectance positions for the arrays with different dopamine concentration. (c) The relationship between luminance and the DA concentration.

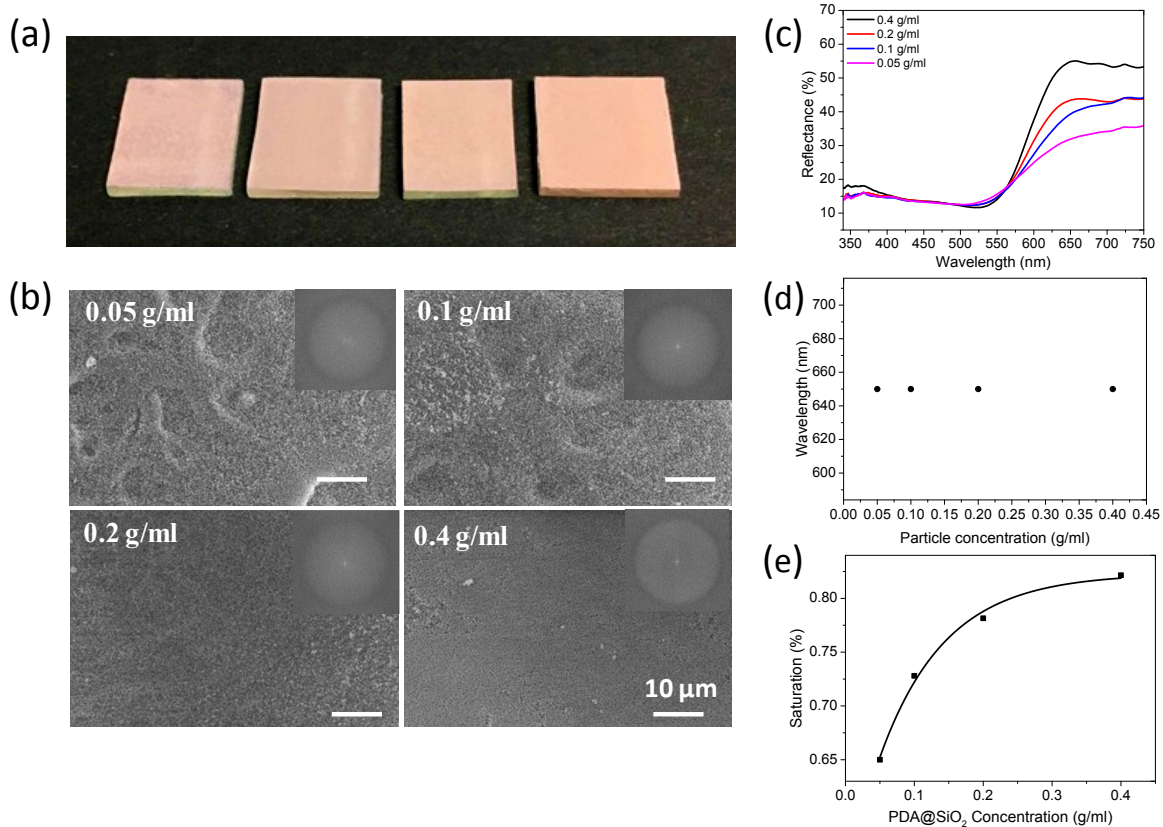


Fig. S16 (a) Photograph of arrays of four saturations, constructed by PDA@SiO₂ concentration with 0.05 g/ml, 0.1 g/ml, 0.2 g/ml and 0.4 g/ml from left to right. (b) SEM images of PDA@SiO₂ distribution on the arrays with four saturations observed under a 600 magnification rate. (c) The reflectance spectrum of the arrays of four PDA@SiO₂ concentration. (d) The reflectance positions for the arrays with different spraying PDA@SiO₂ concentration. (e) The relationship between saturation and the PDA@SiO₂ concentration.

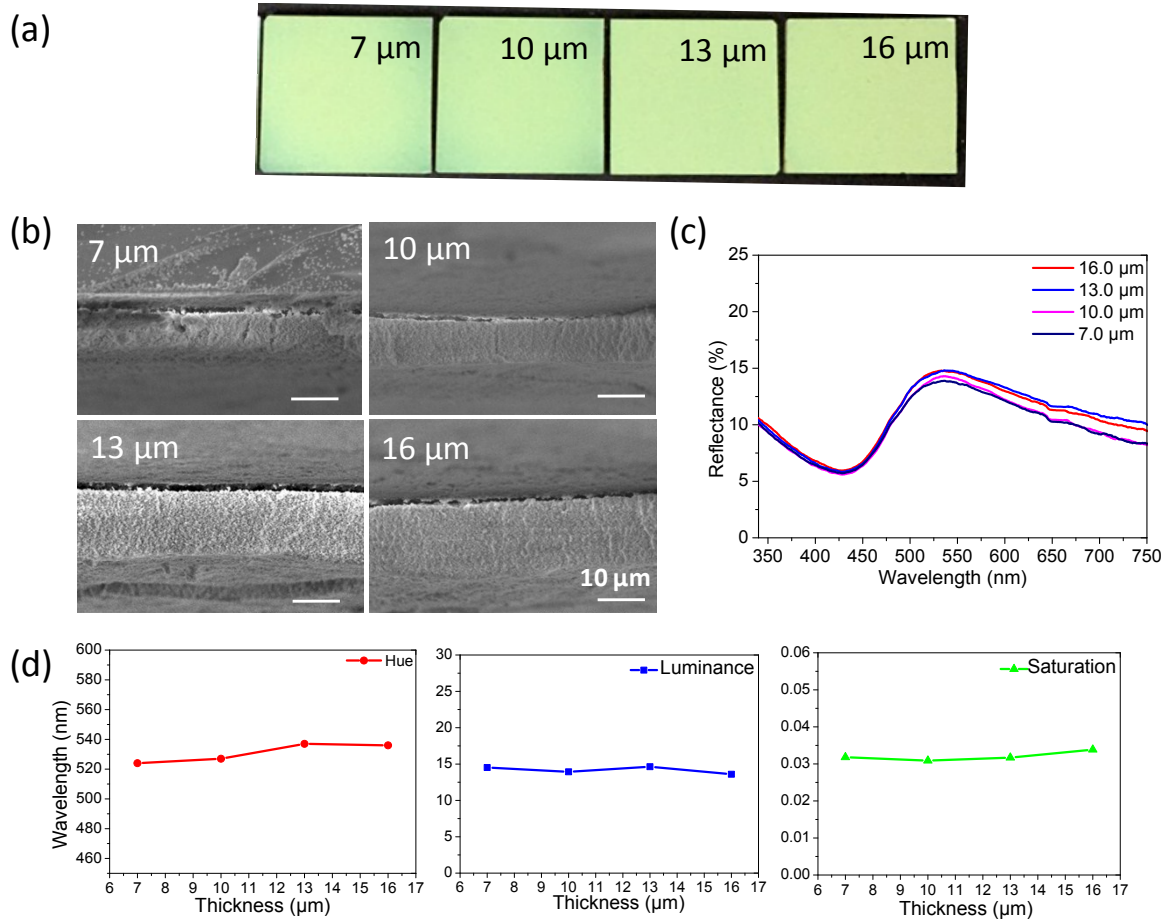


Fig. S17 (a) Photograph of different arrays with 7 μm , 10 μm , 13 μm and 16 μm thickness sprayed by PDA@SiO₂ of 232 nm diameter. (b) SEM image of cross section of the arrays with different thickness. (c) Reflection spectrum of the green arrays with different thickness. (d) The changing curves of the color attributes including Hue, Luminance and Saturation as the increment of thickness.

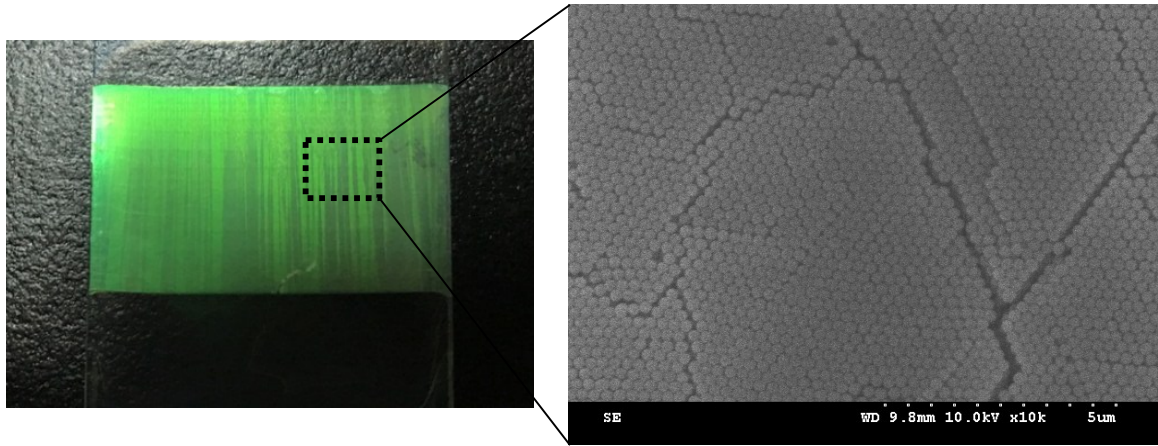


Fig. S18 The image of PDA@SiO₂ colloidal crystal film and the corresponding SEM image of the arrangement with 232 nm particle.

S19. Description of Movies

- **Movie S1** shows the process of spraying PDA@SiO₂ particles with 295 nm size.
- **Movie S2** shows the demonstrate of finger-friction test for PDA@SiO₂-AM arrays on glass, PMMA, paper and Al foil substrates, respectively.
- **Movie S3** shows the performance of SiO₂ arrays, PDA@SiO₂ arrays and PDA@SiO₂-AM arrays with a ultrasonic treatment by a ultrasonic clean instrument with power of 90 W at the bottom of ultrasonic instrument for 35 s.
- **Movie S4** shows the sandpaper abrasion comparative test of SiO₂ arrays, PDA@SiO₂ arrays and PDA@SiO₂-AM arrays on glass substrates.
- **Movie S5** shows the sandpaper abrasion comparative test of SiO₂ arrays, PDA@SiO₂ arrays and PDA@SiO₂-AM arrays on PMMA substrates.
- **Movie S6** shows the sandpaper abrasion comparative test of SiO₂ arrays, PDA@SiO₂ arrays and PDA@SiO₂-AM arrays on Al foils.
- **Movie S7** shows the sandpaper abrasion comparative test of SiO₂ arrays, PDA@SiO₂ arrays and PDA@SiO₂-AM arrays on paper.

References

- [1] S. Rose, A. PrevotEAU, P. Elzière, D. Hourdet, A. Marcellan, L. Leibler, *Nature* 2014, **505**, 382.
- [2] S. Hong, Y. S. Na, S. Choi, I. T. Song, W. Y. Kim, H. Lee, *Adv. Funct. Mater.* 2012, **22**, 4711.
- [3] N. F. D. Vecchia, R. Avolio, M. Alfè, M. E. Errico, A. Napolitano, M. d'Ischia, *Adv. Funct. Mater.* 2013, **23**, 1331.